

Quantization of the thermal Hall conductivity at small Hall angles

Mengxing Ye,^{1,2} Gábor B. Halász,² Lucile Savary,³ and Leon Balents²

¹*School of Physics and Astronomy, University of Minnesota, Minneapolis, Minnesota 55455, USA*

²*Kavli Institute for Theoretical Physics, University of California, Santa Barbara, CA 93106, USA*

³*Université de Lyon, École Normale Supérieure de Lyon, Université Claude Bernard Lyon I,*

CNRS, Laboratoire de physique, 46, allée d'Italie, 69007 Lyon, France

(Dated: October 5, 2018)

We consider the effect of coupling between phonons and a chiral Majorana edge in a gapped chiral spin liquid with Ising anyons (e.g., Kitaev's non-Abelian spin liquid on the honeycomb lattice). This is especially important in the regime in which the longitudinal bulk heat conductivity κ_{xx} due to phonons is much larger than the expected quantized thermal Hall conductance $\kappa_{xy}^q = \frac{\pi T}{12} \frac{k_B^2}{\hbar}$ of the ideal isolated edge mode, so that the thermal Hall angle, i.e., the angle between the thermal current and the temperature gradient, is small. By modeling the interaction between a Majorana edge and bulk phonons, we show that the exchange of energy between the two subsystems leads to a transverse component of the bulk current and thereby an *effective* Hall conductivity. Remarkably, the latter is equal to the quantized value when the edge and bulk can thermalize, which occurs for a Hall bar of length $L \gg \ell$, where ℓ is a thermalization length. We obtain $\ell \sim T^{-5}$ for a model of the Majorana-phonon coupling. We also find that the quality of the quantization depends on the means of measuring the temperature and, surprisingly, a more robust quantization is obtained when the lattice, not the spin, temperature is measured. We present general hydrodynamic equations for the system, detailed results for the temperature and current profiles, and an estimate for the coupling strength and its temperature dependence based on a microscopic model Hamiltonian. Our results may explain recent experiments observing a quantized thermal Hall conductivity in the regime of small Hall angle, $\kappa_{xy}/\kappa_{xx} \sim 10^{-3}$, in α -RuCl₃.

Non-Abelian statistics is a deep generalization of quantum statistics in two dimensions, in which the final state depends upon the order in which exchanges of particles – non-Abelian anyons – are performed [1–3]. In addition to its fundamental interest, this provides a powerful paradigm for quantum computing, allowing for fault-tolerant processes [4, 5]. The main platforms in which non-Abelian topological phases have been sought are the $\nu = 5/2$ Fractional Quantum Hall Effect (FQHE) [1, 2], where non-Abelian anyons are suspected but have not been established, and hybrid semiconductor-superconductor structures, to which quantum computing groups are devoting massive efforts [6], but where confirmation is still awaited.

A third possible route to non-Abelian anyons is via a quantum spin liquid [7]. In his seminal work [8], Kitaev presented a spin-1/2 model on the honeycomb lattice with bond-dependent anisotropy which, in a magnetic field, realizes a non-Abelian topological phase. This phase hosts *Ising anyons*, topologically the same anyon type which is targeted by the hybrid efforts. A key and general characteristic of a topological phase is the *chiral central charge* c , which characterizes its gapless edge modes. It is directly measurable as a quantized thermal Hall conductivity, $\kappa_{xy}^q = \pi c T / 6$ ($\hbar = k_B = 1$). A non-integer value is an unambiguous indicator of a non-Abelian phase, and $c = 1/2$ for Ising anyons.

Stimulated by the recognition that Kitaev's anisotropic interactions arise naturally in certain strongly spin-orbit coupled Mott insulators [9, 10], mounting efforts have targeted such systems in the laboratory. There is now strong evidence that Kitaev interactions are substantial in several 2d honeycomb lattice materials [11]: α -Na₂IrO₃ [12], α -Li₂IrO₃ [13], and α -RuCl₃ [14]. While it is clear that none of these materi-

als are exactly described by Kitaev's model, the beauty of a topological phase is its robustness: once obtained, it is stable to an arbitrary weak perturbation and its essential properties are completely independent of the details of the Hamiltonian. A very recent experiment [15] presents observations of an apparent plateau with a quantized thermal Hall conductivity with $c = 1/2$ in α -RuCl₃ in an applied field of 9-10T, at temperatures of 3-5K. If confirmed, it could be a revolutionary discovery not only in the non-Abelian context, but also as the first truly unambiguous signature of a quantum spin liquid phase in experiment. These results appear to complement recent experiments on quantum Hall systems which have observed half-integer thermal conductance, but through rather different means [16].

The α -RuCl₃ experiments do, however, present at least one major puzzle. The thermal *Hall angle* $\theta_H = \tan^{-1}(\kappa_{xy}/\kappa_{xx}) = 10^{-3}$ is small, i.e., $\kappa_{xx} \gg \kappa_{xy}$. This is incompatible with conduction solely through a Majorana edge mode. Indeed, in two dimensional electron gases, a quantized Hall effect is only observed when the Hall angle is large. This raises the fundamental question of whether the thermal Hall effect is different: is quantization even expected and possible at small Hall angles? We consider here a universal effective model for an Ising anyon phase, in which the chiral Majorana edge mode is augmented by acoustic bulk phonons, which can provide a diagonal bulk thermal conductivity. Remarkably, we find that not only does the quantized thermal Hall effect persist in the presence of the phonons, but it *relies* upon them. The ultimate view of the quantized transport is distinctly different from the usual isolated edge mode picture, and we predict notable experimental consequences of the mixing of edge and bulk heat propagation. Our considerations are quite general

and we expect that similar physics applies to thermal transport in other systems with edge modes, such as topological superconductors and quantum Hall systems.

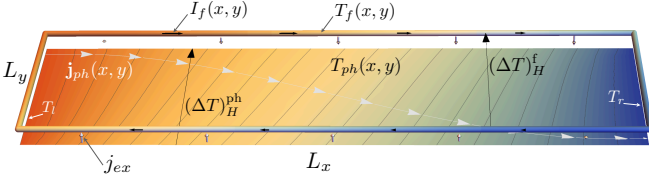


FIG. 1. Temperature maps of our rectangular system with dimensions L_x and L_y consisting of a phonon bulk (lower box) and a Majorana fermion edge (upper edge). The phonon temperatures at the left and right edges are assumed to be fixed as $T_{l,r}$, respectively, due to the coupling of the lattice with the heater and thermal bath. The black arrows for I_f along the edge denote the direction and magnitude of the “clockwise” energy current associated with the chiral Majorana mode. The white arrows in the bulk show a stream line of \mathbf{j}_{ph} . The 3d white arrows for j_{ex} indicate the energy current between the Majorana edge and bulk phonons. $(\Delta T)_H^{ph}$ and $(\Delta T)_H^f$ are the measured “Hall” temperature differences when the contacts are coupled to the lattice or spins, respectively.

We formulate the problem in terms of hydrodynamic equations describing the energy transport. We consider the following two subsystems: the phonons, or lattice, located in the bulk, and denoted with the index “ ph ”, and the Majorana fermions, or spins, confined to the edge and indexed by “ f ”, as well as a coupling between them. For simplicity, we assume an isotropic bulk, with the relation

$$\mathbf{j}_{ph} = -\kappa \nabla T_{ph}, \quad (1)$$

i.e., the energy current density in the bulk is parallel to the thermal gradient, with κ a characteristic of the lattice. The “clockwise” edge current is that of a chiral fermion with central charge $c = 1/2$, i.e.,

$$I_f = \frac{\pi c T_f^2}{12}. \quad (2)$$

The heat exchange between the phonons and Majoranas can be modeled phenomenologically through an energy current j_{ex} between the two subsystems (see the arrows in Fig. 1). Microscopically, it is due to the scattering events between edge Majorana fermions and bulk phonons, and is the rate of energy transfer at the edge per unit length, i.e., $j_{ex} \equiv \frac{1}{L} \left(\frac{\partial \mathcal{E}}{\partial t} \right)_{ph \rightarrow f} = -\frac{1}{L} \left(\frac{\partial \mathcal{E}}{\partial t} \right)_{f \rightarrow ph}$, where L is the length of the edge in evaluating $\left(\frac{\partial \mathcal{E}}{\partial t} \right)_{f \rightarrow ph}$ [17]. This in turn implies that the phonons and Majoranas have not fully thermalized with one another. Assuming, however, that thermalization is almost complete, i.e., $T_f \approx T_{ph}$, and that the fermions are strictly confined to the edge, j_{ex} can be linearized in the temperature difference $T_{ph} - T_f$ at the edge,

$$j_{ex} = \lambda(T)(T_{ph} - T_f), \quad (3)$$

where, crucially, $\lambda > 0$ is a function of the overall constant temperature $T \approx T_{ph,f}$, and can be parametrized as $\lambda(T) \sim$

T^α . We will determine α from a phase space analysis of the scattering events.

Hydrodynamic equations.—We assume our (two-dimensional) system to be a rectangular slab of width L_y and length $L_x \gtrsim L_y$ (see Fig. 1), and choose coordinates with $|x| < x_0 = L_x/2$ and $|y| < y_0 = L_y/2$.

The continuity equation in the bulk in a steady state is $\nabla \cdot \mathbf{j}_{ph}(x, y) = 0$ which implies the Laplace equation

$$\nabla^2 T_{ph}(x, y) = 0. \quad (4)$$

Energy conservation at the edges gives rise to appropriate boundary conditions. At the left and right edges, we assume that only the *lattice* is coupled to thermal leads and the phonons have fixed constant temperatures, $T_{l,r}$, respectively. At the top and bottom edges, the current out of the phonon subsystem must equal the exchange current, hence $\pm j_{ph}^y(x, \pm y_0) = j_{ex}(x, \pm y_0)$. Moreover, the continuity equations for the edges imply $\pm \partial_x I_f(x, \pm y_0) = j_{ex}(x, \pm y_0)$. Together these yield, given Eqs. (1) and (2),

$$\kappa \partial_y T_{ph}(x, \pm y_0) = -\kappa_{xy}^q \partial_x T_f(x, \pm y_0). \quad (5)$$

Note the appearance of the ideal quantized Hall conductivity $\kappa_{xy}^q = \pi c T / 6 = \pi T / 12$ here, using $T_f \approx T$ (valid within our linearized treatment).

Quantization in the infinitely long limit.—For simplicity, we first solve our hydrodynamic equations in the limit of an infinitely long system ($L_x \rightarrow \infty$). Note that, even for finite systems with $L_x \gg L_y$, this infinitely long limit is expected to be relevant far away from the left and right edges.

Since there is translation symmetry in the x direction, the boundary conditions $T_{ph}(\pm x_0, y) = T_{r,l}$ lead to a uniform temperature gradient $\frac{dT}{dx} = \lim_{L_x \rightarrow \infty} \frac{T_r - T_l}{L_x}$, and the phonon and Majorana temperatures must take the forms

$$\begin{cases} T_{ph}(x, y) = \frac{dT}{dx} x + \hat{T}(y) + \text{const.} \\ T_f(x, \pm y_0) = \frac{dT}{dx} x + \text{const.} \end{cases} \quad (6)$$

Laplace’s equation, Eq. (4), immediately implies that $\hat{T}(y)$ must be a linear function of y which we write $\hat{T}(y) = \frac{(\Delta T)_H^{ph}}{L_y} y$. Therefore, from Eq. (5), we get

$$\partial_y T_{ph}(x, y) = -\frac{\kappa_{xy}^q}{\kappa} \frac{dT}{dx}, \quad (7)$$

since $\partial_y T_{ph}(x, y) = \partial_y T_{ph}(x, \pm y_0) = \text{const.}$. From a phenomenological perspective, the *total* current in the Hall bar geometry must flow only along x , but Eq. (7) implies that the phonon thermal gradient is tilted from the current axis by a small Hall angle of $|\tan \theta_H| = \kappa_{xy}^q / \kappa \ll 1$.

Next consider the view of Alice the experimentalist. She measures the temperature gradients via three contacts, and assumes for the moment that these measurements give the phonon temperature (the most reasonable assumption). To deduce the Hall conductivity, she posits a bulk heat current

satisfying $\mathbf{j} = -\kappa^{\text{ph,expt}} \cdot \nabla T$, and tries to deduce the tensor $\kappa^{\text{ph,expt}}$ [the $ph(f)$ superscript means this quantity is obtained from a measurement of the phonon (Majorana fermion) temperature]. By measuring the longitudinal temperature gradient, she obtains $\kappa_{xx}^{\text{ph,expt}} = \kappa$ as expected, and then, imposing $j^y = 0$, she equates the experimental Hall angle $\tan \theta_H = \frac{(\Delta T)_H^{\text{ph}}}{L_y} \frac{dT}{dx}$ to $\kappa_{xy}^{\text{ph,expt}} / \kappa_{xx}^{\text{ph,expt}}$. By comparing this equation to the theoretical result in Eq. (7), we immediately recognize that the magnitude of the effective Hall conductivity (denoted simply as $\kappa_{xy}^{\text{expt}}$ in the rest of the text) is $|\kappa_{xy}^{\text{ph,expt}}| = \kappa_{xy}^q$, i.e., the experimentally measured thermal Hall conductivity takes the quantized value!

A few remarks are in order. First, a transverse temperature difference, $(\Delta T)_H^{\text{ph}}$, leading to a ‘‘Hall thermal gradient’’ $(\Delta T)_H^{\text{ph}} / L_y = -\frac{\kappa_{xy}^q}{\kappa} \frac{dT}{dx}$ develops which allows to compensate the transverse energy current j_{ex} at the edges and leads to a zero net transverse current. Second, the effective thermal Hall conductivity is only found to be quantized if the transverse temperature gradient is obtained from the *phonon* temperatures at the top and bottom edges. In contrast, if Bob somehow measures the Majorana temperatures, the transverse temperature gradient is identified as $(\Delta T)_H^f / L_y$ and thus, from Eqs. (3) and (5), he finds a different effective thermal Hall conductivity [see also Fig. 2(a)]:

$$\kappa_{xy}^{\text{f,expt}} = -\frac{\kappa(\Delta T)_H^f}{L_y \frac{dT}{dx}} = \kappa_{xy}^q \left(1 + \frac{2\kappa}{\lambda(T)L_y} \right). \quad (8)$$

Note that $\kappa_{xy}^{\text{f,expt}} \approx \kappa_{xy}^{\text{ph,expt}}$ only for a large enough phonon-Majorana coupling $\lambda(T) \gg \kappa / L_y$.

General conditions for quantization.—To understand how the quantization of the effective thermal Hall conductivity can break down and determine the range of its applicability, we now extend the solution of our hydrodynamic equations to a finite system with $L_x \gtrsim L_y$, where we must take into account all boundary conditions, i.e., include the right and left boundary conditions on top of those in Eq. (5). Again assuming that the leads are coupled to the phonons only, those are:

$$\begin{cases} T_{ph}(\pm x_0, y) = T_{r,l}, \\ j_{ex}(\pm x_0, y) = \lambda(T)(T_{ph} - T_f) = \mp \kappa_{xy}^q \partial_y T_f. \end{cases} \quad (9)$$

Considering a small enough phonon-Majorana coupling λ , we aim to obtain a perturbative solution of the hydrodynamic equations. To this end, we write

$$T_{ph,f}(x, y) = T + \tilde{T}_{ph,f}(x, y), \quad (10)$$

with $\tilde{T}_{ph,f}(x, y) \ll T$. We express the temperature variations in series expansions as $\tilde{T}_{ph,f} = \sum_{n=0}^{\infty} \tilde{T}_{ph,f}^{(n)}$ and assume that terms of increasing order n are progressively less important. Note also that $\tilde{T}_{ph,f}(x, y) = -\tilde{T}_{ph,f}(-x, -y)$ generally follows from the symmetries of the hydrodynamic equations. Starting from the $\lambda = 0$ solution, $\tilde{T}_{ph}^{(0)}(x, y) = \frac{dT}{dx}x$ and $\tilde{T}_f^{(0)}(x, y) = 0$, the temperature variations can then be

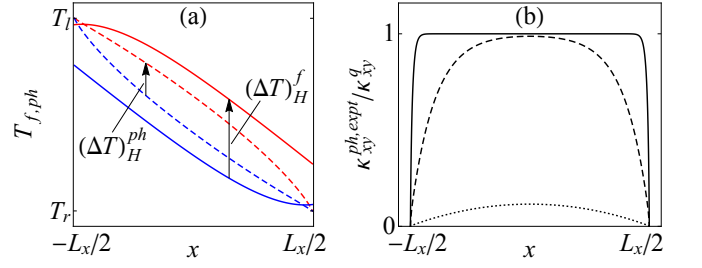


FIG. 2. (a) Temperature profiles of the Majorana fermions (solid lines) and phonons (dashed lines) at the top (red lines) and bottom (blue lines) edges, $T_{f,ph}(x, \pm y_0)$. The measured ‘‘Hall’’ temperature differences $(\Delta T)_H^{\text{ph},f}(x) \equiv T_{ph,f}(x, y_0) - T_{ph,f}(x, -y_0)$ are shown with the black arrows. (b) Measured thermal Hall conductivity $\kappa_{xy}^{\text{ph,expt}}$ [Eq. (13)] as a function of the longitudinal position x at which $(\Delta T)_H^{\text{ph}}$ is measured for dimensionless thermal couplings $\lambda L_x / \kappa_{xy}^q = 100$ (solid line), 10 (dashed line), and 1 (dotted line) at fixed $L_x / L_y = 100$.

found by an iterative procedure. At each iteration step $n > 0$, we first solve the ordinary differential equations [see Eqs. (5) and (9)]

$$\begin{aligned} \kappa_{xy}^q \partial_x \tilde{T}_f^{(n)} &= \pm \lambda \left[\tilde{T}_{ph}^{(n-1)} - \tilde{T}_f^{(n)} \right] & \text{for } y = \pm y_0, \\ \kappa_{xy}^q \partial_y \tilde{T}_f^{(n)} &= \mp \lambda \left[\tilde{T}_{ph}^{(n-1)} - \tilde{T}_f^{(n)} \right] & \text{for } x = \pm x_0, \end{aligned} \quad (11)$$

for the Majorana temperature $\tilde{T}_f^{(n)}$ along the edge. Then, using this solution, we obtain an appropriate Laplace equation $\nabla^2 \tilde{T}_{ph}^{(n)} = 0$ for the phonon temperature $\tilde{T}_{ph}^{(n)}$ in the bulk, along with Dirichlet boundary conditions $\tilde{T}_{ph}^{(n)}(\pm x_0, y) = 0$ at the left and right edges, and Neumann boundary conditions

$$\partial_y \tilde{T}_{ph}^{(n)} = \pm \frac{\lambda}{\kappa} \left[\tilde{T}_f^{(n)} - \tilde{T}_{ph}^{(n-1)} \right] & \text{for } y = \pm y_0, \quad (12)$$

at the top and bottom edges. It is well known that such a Laplace equation with mixed Dirichlet and Neumann boundary conditions has a unique solution that can be obtained by standard methods. Our perturbative solution is convergent whenever $\lambda \ll \kappa / L_y$ (see [18] for the error analysis).

Assuming this condition, we perform the first iteration step (see [18]) to calculate the phonon temperature $\tilde{T}_{ph}^{(1)}$ and obtain the effective thermal Hall conductivity in terms of the transverse temperature difference $(\Delta T)_H^{\text{ph}}(x)$ [see Fig. 2(a)]:

$$\kappa_{xy}^{\text{ph,expt}}(x) = -\frac{\kappa}{\frac{dT}{dx} L_y} \left[\tilde{T}_{ph}^{(1)}(x, y_0) - \tilde{T}_{ph}^{(1)}(x, -y_0) \right]. \quad (13)$$

Note that $\kappa_{xy}^{\text{ph,expt}}(x)$ generally depends on the position x at which the temperatures are measured [see Fig. 2(b)]. Indeed, we find that $\kappa_{xy}^{\text{ph,expt}}(x)$ only takes a quantized (or even constant) value if $L_x \gg L_y$ and $L_x \gg \ell \equiv \kappa_{xy}^q / \lambda$. First, an accurate measurement of the thermal Hall conductivity generally requires an elongated system with $L_x \gg L_y$. Second, the system size L_x must be larger than the characteristic length ℓ associated with the thermalization of the Majorana edge mode

(see Table I for a summary). Indeed, even for $L_x \gg L_y$, there are two regimes for the effective thermal Hall conductivity (see [18]):

$$\kappa_{xy}^{\text{ph,expt}}(x) \approx \begin{cases} \frac{\pi T}{12} & (L_x \gg \ell), \\ \frac{\pi T(L_x^2 - 4x^2)}{96\ell^2} & (L_x \ll \ell). \end{cases} \quad (14)$$

In the second regime we find that $\kappa_{xy}^{\text{ph,expt}}(x)$ has a strong dependence on x and is smaller than $\kappa_{xy}^q = (\pi/12)T$ by a factor $\sim (L_x/\ell)^2 \ll 1$.

Estimation of the spin-lattice thermal coupling λ .—The phenomenological spin-lattice coupling $\lambda(T)$ defined in Eq. (3) can be obtained microscopically from, e.g., the Boltzmann equation. We calculate the rate of energy exchange per unit length $j_{ex} = \frac{1}{L} \left(\frac{\partial \mathcal{E}}{\partial t} \right)_{ph \rightarrow f}$ due to the scattering at the edge. Comparing to the form in Eq. (3), we extract $\lambda(T) = \lambda_0 T^\alpha$, i.e., the exponent α and the coefficient λ_0 .

We consider a coupling at the top edge $y = y_0 = L_y/2$ of the form

$$H_{int} = \frac{-igv_f}{4} \int dx \zeta(x) K_{ij} \partial_i u_j(x, y_0) \eta(x) \partial_x \eta(x), \quad (15)$$

where $\eta(x)$, $\vec{u}(x, y)$, $\zeta(x)$ are the Majorana edge mode, the lattice displacement field, and disorder potential, respectively, g parametrizes the spin-lattice coupling, and v_f is the fermion velocity. $K_{ij} \partial_i u_j$ with $i, j = x, y$ is some linear combination of the elastic tensor for u . Physically, Eq. (15) may be understood from the observation that the lattice displacement modifies the velocity of the Majorana edge mode by affecting the strength of the Kitaev coupling.

Using Eq. (15) and calculating the energy transfer rate using a Boltzmann equation, we obtain a large power $\alpha = 6$. The reason for the large exponent is twofold. First, the dispersions of both bulk phonons and edge Majoranas are linear which reduces the low energy phase space. Second, the vertex necessarily involves two gradients: one because $\eta(x)\eta(x) = \delta(0)$ is a c-number for Majorana fermions, and another because the strain tensor includes a gradient. We note that, without disorder, two-phonon processes are necessary to satisfy kinematic constraints in the physical regime, where the velocity of the acoustic phonon v_{ph} is larger than v_f . In that case one obtains an even larger $\alpha = 8$.

To estimate the coefficient λ_0 , we further assume that the averaged disorder potential satisfies $\langle \zeta(x)\zeta(x') \rangle_{dis} = \zeta^2 \delta(x - x')$, and consider an isotropic acoustic phonon mode only. From the Boltzmann equation solution (see [18]), we obtain

$$\lambda = \frac{g^2 \zeta^2}{32(2\pi)^3 v_{ph}^4 v_f^2 \rho_0} f T^6, \quad (16)$$

where ρ_0 is the mass density of the lattice. In the model we consider, $f = 4.2 \times 10^4$. Unfortunately, at this time an accurate quantitative estimate of λ for α -RuCl₃ is not possible due to the lack of knowledge of microscopic details of g , v_f

and ζ . However, crudely applying Eq. (16), we estimate the characteristic length $\ell = \kappa_{xy}^q/\lambda$ to be several orders of magnitude larger than the lattice spacing at temperatures of a few Kelvins. Importantly, due to the large exponent α , we expect that upon lowering the temperature of the sample, ℓ grows rapidly and that the system enters the regime where $L_x \ll \ell$ in Eq. (14) and thus the quantization of the thermal Hall conductivity breaks down.

Summary and discussion.—By carefully analyzing the interplay between the chiral Majorana edge mode of an Ising anyon phase and the energy currents carried by bulk phonons, we have demonstrated that the thermal Hall conductivity of such a non-Abelian topological phase can be effectively quantized in the presence of a much larger longitudinal thermal conductivity. This is in accordance with recent experiments on α -RuCl₃ [15]. However, this quantization only survives under certain conditions. The main results are summarized in Table I.

Coupling regime	Weak	Intermediate	Strong
$\lambda \sim T^\alpha$	$\lambda \lesssim \lambda_f$	$\lambda_f \ll \lambda \ll \lambda_{ph}$	$\lambda_{ph} \ll \lambda$
L_x	$L_x \lesssim \ell$		$L_x \gg \ell$
L_y		$L_y \ll \kappa/\lambda$	$L_y \gg \kappa/\lambda$
$\kappa_{xy}^{\text{ph,expt}}$	$\kappa_{xy}^{\text{ph,expt}} \ll \kappa_{xy}^q$	κ_{xy}^q	κ_{xy}^q
$\kappa_{xy}^{\text{f,expt}}$	—[19]	$\kappa_{xy}^{\text{f,expt}} \gg \kappa_{xy}^q$	κ_{xy}^q

TABLE I. Values of the effective thermal Hall conductivities extracted by measuring the temperatures of the phonon ($\kappa_{xy}^{\text{ph,expt}}$) or Majorana ($\kappa_{xy}^{\text{f,expt}}$) subsystems in three coupling regimes, defined by the value of λ relative to $\lambda_f = \kappa_{xy}^q/L_x$ and $\lambda_{ph} = \kappa/L_y$. The three coupling regimes can also be identified by comparing the system dimensions L_x , L_y to the characteristic lengths $\ell = \kappa_{xy}^q/\lambda$ and κ/λ .

In words, those results are as follows. The quantization survives for a sufficiently strong spin-lattice coupling $\lambda \gg \lambda_f \equiv \kappa_{xy}^q/L_x$, while it immediately disappears in the weak-coupling regime defined by $\lambda \lesssim \lambda_f$ [see Fig. 2(b)]. Importantly, since $\lambda \propto T^\alpha$ is strongly dependent on the temperature, with $\alpha \geq 6$ for the mechanisms considered in this work, we predict that the observed quantization of the thermal Hall conductivity should eventually break down as the temperature is lowered.

Even within the range of quantization ($\lambda \gg \lambda_f$), we can identify two separate regimes, depending on how λ compares to $\lambda_{ph} \equiv \kappa/L_y \gg \lambda_f$. In the strong-coupling regime, defined by $\lambda \gg \lambda_{ph}$, the spins and the lattice share the same temperature, and the quantization of the thermal Hall conductivity follows from effectively having a system with a diagonal conductivity $\kappa_{xx}^{\text{expt}} = \kappa_{yy}^{\text{expt}} = \kappa$ of the phonons and an off-diagonal $\kappa_{xy}^{\text{expt}} = \kappa_{xy}^q$ of the Majoranas. Surprisingly, however, in the intermediate regime defined by $\lambda_f \ll \lambda \ll \lambda_{ph}$, the thermal Hall conductivity appears to be quantized *despite* a large temperature mismatch between the spins and the lat-

tice. This is only true, however, if it is obtained by measuring the *lattice* temperatures along the edge. If one could directly measure the local temperature of the Majorana edge mode, it would appear to give a much larger thermal Hall conductivity.

Finally, we emphasize that our hydrodynamic equations are applicable far beyond the scope of the present work. Here, by solving them, we obtained a wide range of experimentally measurable quantities, such as detailed temperature profiles of various degrees of freedom (e.g., spins and lattice) across the system. However, due to their phenomenological nature, the hydrodynamic equations we derived should readily extend to a rich variety of chiral topological phases and thus may find applications far away from the field of quantum spin liquids.

L. B. was supported by the DOE Office of Science’s Basic Energy Sciences program under Award No. DE-FG02-08ER46524. M. Y. acknowledges support from the KITP graduate fellowship program under Grant No. NSF PHY-1748958 and the NSF DMR-1523036 from the University of Minnesota. G. B. H. is supported by the Gordon and Betty Moore Foundation’s EPiQS Initiative through Grant No. GBMF4304.

[1] G. Moore and N. Read, Nuclear Physics B **360**, 362 (1991).
 [2] N. Read and D. Green, Physical Review B **61**, 10267 (2000).
 [3] F. Wilczek, in *The Spin*, Vol. 55, edited by B. Duplantier, J. Raimond, and V. Rivasseau (Progress in Mathematical Physics, Birkhäuser Basel, 2009).
 [4] A. Y. Kitaev, Annals of Physics **303**, 2 (2003).
 [5] C. Nayak, S. H. Simon, A. Stern, M. Freedman, and S. D. Sarma, Reviews of Modern Physics **80**, 1083 (2008).
 [6] R. M. Lutchyn, E. P. A. M. Bakkers, L. P. Kouwenhoven, P. Krogstrup, C. M. Marcus, and Y. Oreg, Nature Reviews Ma-

terials **3**, 52 (2018).
 [7] L. Savary and L. Balents, Reports on Progress in Physics **80**, 016502 (2017).
 [8] A. Kitaev, Annals of Physics **321**, 2 (2006).
 [9] G. Jackeli and G. Khaliullin, Physical review letters **102**, 017205 (2009).
 [10] S. Trebst, arXiv preprint arXiv:1701.07056 (2017).
 [11] S. M. Winter, Y. Li, H. O. Jeschke, and R. Valentí, Phys. Rev. B **93**, 214431 (2016).
 [12] S. H. Chun, J.-W. Kim, J. Kim, H. Zheng, C. C. Stoumpos, C. Malliakas, J. Mitchell, K. Mehlawat, Y. Singh, Y. Choi, *et al.*, Nature Physics **11**, 462 (2015).
 [13] S. Williams, R. Johnson, F. Freund, S. Choi, A. Jesche, I. Kimchi, S. Manni, A. Bombardi, P. Manuel, P. Gegenwart, *et al.*, Physical Review B **93**, 195158 (2016).
 [14] K. W. Plumb, J. P. Clancy, L. J. Sandilands, V. V. Shankar, Y. F. Hu, K. S. Burch, H.-Y. Kee, and Y.-J. Kim, Phys. Rev. B **90**, 041112 (2014).
 [15] Y. Kasahara, T. Ohnishi, Y. Mizukami, O. Tanaka, S. Ma, K. Sugii, N. Kurita, H. Tanaka, J. Nasu, Y. Motome, T. Shibauchi, and Y. Matsuda, Nature **559**, 227 (2018).
 [16] M. Banerjee, M. Heiblum, V. Umansky, D. E. Feldman, Y. Oreg, and A. Stern, Nature **559**, 205 (2018).
 [17] Note that $L = L_x$, resp. $L = L_y$, for j_{ex} (top/bottom), resp. j_{ey} (left/right).
 [18] Supplementary Material.
 [19] “-” in the last line means that the quantization $\kappa_{xy}^{f,\text{expt}}$ relative to κ_{xy}^q is not generic ($\kappa_{xy}^{f,\text{expt}} \gtrsim \kappa_{xy}^q$) in the weak coupling regime $\lambda \lesssim \lambda_f$, i.e., it depends on the strength of λ and the position x where the temperature is measured.
 [20] N. Ashcroft and N. Mermin, *Solid State Physics*, HRW international editions (Holt, Rinehart and Winston, 1976).
 [21] Using the Fourier transform definition $\eta(x) = \sqrt{\frac{2}{L_x}} \sum_{k \geq 0} (\eta_k e^{ikx} + \eta_k^\dagger e^{-ikx})$ where the sum runs only over positive momenta, we obtain the same results.
 [22] The same conclusion can be obtained by calculating the matrix element diagrammatically [see Fig. 3(b)] from the couplings of Eq. (46).

SUPPLEMENTARY MATERIAL

First-order solution of the hydrodynamic equations

Here we work out the first iteration step of the perturbative solution described in the main text and use it to determine the effective thermal Hall conductivity $\kappa_{xy}^{\text{ph,expt}}(x)$ as a function of the longitudinal position x . At the first iteration step ($n = 1$), the ordinary differential equations for the Majorana temperature $\tilde{T}_f^{(1)}(x, y)$ in Eq. (11) of the main text are

$$\begin{aligned}\partial_x \tilde{T}_f^{(1)}\left(x, \pm \frac{L_y}{2}\right) &= \pm \frac{1}{\ell} \left[\tilde{T}_{ph}^{(0)}\left(x, \pm \frac{L_y}{2}\right) - \tilde{T}_f^{(1)}\left(x, \pm \frac{L_y}{2}\right) \right], \\ \partial_y \tilde{T}_f^{(1)}\left(\pm \frac{L_x}{2}, y\right) &= \mp \frac{1}{\ell} \left[\tilde{T}_{ph}^{(0)}\left(\pm \frac{L_x}{2}, y\right) - \tilde{T}_f^{(1)}\left(\pm \frac{L_x}{2}, y\right) \right],\end{aligned}\quad (17)$$

where $\ell = \kappa_{xy}^q/\lambda$ is the characteristic thermalization length of the Majorana edge mode. Remembering that $\tilde{T}_{ph}^{(0)}(x, y) = \frac{dT}{dx}x$, the solutions of Eq. (17) at the left and top edges become

$$\begin{aligned}\tilde{T}_f^{(1)}\left(-\frac{L_x}{2}, y\right) &= -\frac{dT}{dx} \left\{ \frac{L_x}{2} - \frac{\ell[1 - e^{-L_x/\ell}]}{1 + e^{-(L_x+L_y)/\ell}} \exp\left[-\frac{y + L_y/2}{\ell}\right] \right\}, \\ \tilde{T}_f^{(1)}\left(x, \frac{L_y}{2}\right) &= -\frac{dT}{dx} \left\{ (\ell - x) - \frac{\ell[1 + e^{-L_y/\ell}]}{1 + e^{-(L_x+L_y)/\ell}} \exp\left[-\frac{x + L_x/2}{\ell}\right] \right\},\end{aligned}\quad (18)$$

while those at the right and bottom edges are related by the symmetry constraint $\tilde{T}_f^{(1)}(x, y) = -\tilde{T}_f^{(1)}(-x, -y)$. Laplace's equation $\nabla^2 \tilde{T}_{ph}^{(1)}(x, y) = 0$ for the phonon temperature $\tilde{T}_{ph}^{(1)}(x, y)$ is then supplemented with the Dirichlet boundary conditions $\tilde{T}_{ph}^{(1)}(\pm L_x/2, y) = 0$ at the left and right edges and the Neumann boundary conditions [see Eq. (12) in the main text]

$$\begin{aligned}\partial_y \tilde{T}_{ph}^{(1)}\left(x, \pm \frac{L_y}{2}\right) &= \pm \frac{\lambda}{\kappa} \left[\tilde{T}_f^{(1)}\left(x, \pm \frac{L_y}{2}\right) - \tilde{T}_{ph}^{(0)}\left(x, \pm \frac{L_y}{2}\right) \right] \\ &= \frac{-\frac{dT}{dx} \kappa_{xy}^q}{\kappa} \left[1 - \frac{1 + e^{-L_y/\ell}}{1 + e^{-(L_x+L_y)/\ell}} \exp\left(-\frac{L_x/2 \pm x}{\ell}\right) \right]\end{aligned}\quad (19)$$

at the top and bottom edges. It is well known that Laplace's equation with such boundary conditions has a unique solution. After the iteration step $n = 1$, the only error in the temperature corrections $\tilde{T}_{ph}^{(1)}$ and $\tilde{T}_f^{(1)}$ is due to the absence of $\tilde{T}_{ph}^{(1)}$ on the right-hand sides of Eqs. (17) and (19). Indeed, including this term would precisely give rise to the next temperature corrections $\tilde{T}_{ph}^{(2)}$ and $\tilde{T}_f^{(2)}$. The same type of error from $\tilde{T}_{ph}^{(n)}$ persists in the same way at a given iterative step n . However, it follows from Eq. (19) [see also Eq. (12)] that successive temperature corrections $\tilde{T}_{ph}^{(n)}$ are progressively less important and hence our perturbative solution is convergent whenever $\lambda \ll \kappa/L_y$. Surprisingly, as long as $\kappa_{xy}^q \ll \kappa$, the perturbative solution is actually valid for an *arbitrary* value of λ . Indeed, at $\lambda \rightarrow \infty$, one can formulate an equivalent perturbative solution for $\tilde{T}_{ph} = \tilde{T}_f$ at the edges in which the small parameter is manifestly κ_{xy}^q/κ .

Recalling the symmetry constraint $\tilde{T}_{ph}^{(1)}(x, y) = -\tilde{T}_{ph}^{(1)}(-x, -y)$, we search for this solution in the general form

$$\tilde{T}_{ph}^{(1)}(x, y) = \sum_{m=1}^{\infty} \left\{ A_m \cos\left[\frac{(2m-1)\pi x}{L_x}\right] \sinh\left[\frac{(2m-1)\pi y}{L_x}\right] + B_m \sin\left[\frac{2m\pi x}{L_x}\right] \cosh\left[\frac{2m\pi y}{L_x}\right] \right\}, \quad (20)$$

which automatically satisfies the Dirichlet boundary conditions. To find independent equations for the coefficients A_m and B_m ,

we take symmetric and antisymmetric combinations of the Neumann boundary conditions in Eq. (19):

$$\begin{aligned}
\partial_y \tilde{T}_{ph}^{(1)}\left(x, \frac{L_y}{2}\right) + \partial_y \tilde{T}_{ph}^{(1)}\left(x, -\frac{L_y}{2}\right) &= \frac{-2\frac{dT}{dx}\kappa_{xy}^q}{\kappa} \left\{ 1 - \frac{1 + e^{-L_y/\ell}}{1 + e^{-(L_x+L_y)/\ell}} \exp\left(-\frac{L_x}{2\ell}\right) \cosh \frac{x}{\ell} \right\} \\
&= \sum_{m=1}^{\infty} \frac{2(2m-1)\pi A_m}{L_x} \cos\left[\frac{(2m-1)\pi x}{L_x}\right] \cosh\left[\frac{(2m-1)\pi L_y}{2L_x}\right], \\
\partial_y \tilde{T}_{ph}^{(1)}\left(x, \frac{L_y}{2}\right) - \partial_y \tilde{T}_{ph}^{(1)}\left(x, -\frac{L_y}{2}\right) &= \frac{-2\frac{dT}{dx}\kappa_{xy}^q[1 + e^{-L_y/\ell}]}{\kappa[1 + e^{-(L_x+L_y)/\ell}]} \exp\left(-\frac{L_x}{2\ell}\right) \sinh \frac{x}{\ell} \\
&= \sum_{m=1}^{\infty} \frac{4m\pi B_m}{L_x} \sin\left[\frac{2m\pi x}{L_x}\right] \sinh\left[\frac{m\pi L_y}{L_x}\right].
\end{aligned} \tag{21}$$

From Eq. (21), the individual coefficients A_m and B_m in Eq. (20) are

$$\begin{aligned}
A_m &= \frac{-\frac{dT}{dx}L_x\kappa_{xy}^q}{(2m-1)\pi\kappa} \operatorname{sech}\left[\frac{(2m-1)\pi L_y}{2L_x}\right] \mathcal{I}_m, \\
B_m &= \frac{-\frac{dT}{dx}L_x\kappa_{xy}^q}{2m\pi\kappa} \operatorname{cosech}\left[\frac{m\pi L_y}{L_x}\right] \mathcal{J}_m,
\end{aligned} \tag{22}$$

where the Fourier integrals \mathcal{I}_m and \mathcal{J}_m take the forms

$$\begin{aligned}
\mathcal{I}_m &= \frac{2}{L_x} \int_{-L_x/2}^{L_x/2} d\tilde{x} \cos\left[\frac{(2m-1)\pi\tilde{x}}{L_x}\right] \left\{ 1 - \frac{1 + e^{-L_y/\ell}}{1 + e^{-(L_x+L_y)/\ell}} \exp\left(-\frac{L_x}{2\ell}\right) \cosh \frac{\tilde{x}}{\ell} \right\}, \\
\mathcal{J}_m &= \frac{2}{L_x} \int_{-L_x/2}^{L_x/2} d\tilde{x} \sin\left[\frac{2m\pi\tilde{x}}{L_x}\right] \frac{1 + e^{-L_y/\ell}}{1 + e^{-(L_x+L_y)/\ell}} \exp\left(-\frac{L_x}{2\ell}\right) \sinh \frac{\tilde{x}}{\ell}.
\end{aligned} \tag{23}$$

From Eqs. (20) and (22), the effective thermal Hall conductivity in Eq. (13) of the main text is then

$$\begin{aligned}
\kappa_{xy}^{\text{ph,expt}}(x) &= \frac{\kappa}{-\frac{dT}{dx}L_y} \left[\tilde{T}_{ph}^{(1)}\left(x, \frac{L_y}{2}\right) - \tilde{T}_{ph}^{(1)}\left(x, -\frac{L_y}{2}\right) \right] \\
&= \sum_{m=1}^{\infty} \frac{2L_x\kappa_{xy}^q}{(2m-1)\pi L_y} \tanh\left[\frac{(2m-1)\pi L_y}{2L_x}\right] \cos\left[\frac{(2m-1)\pi x}{L_x}\right] \mathcal{I}_m.
\end{aligned} \tag{24}$$

In the limit of $L_x \gg L_y$, we can expand the function $\tanh[(2m-1)\pi L_y/2L_x]$ up to first order in L_y/L_x and use the completeness of the Fourier functions $\cos[(2m-1)\pi x/L_x]$ to obtain a more tractable (but approximate) expression:

$$\kappa_{xy}^{\text{ph,expt}}(x) = \kappa_{xy}^q \sum_{m=1}^{\infty} \cos\left[\frac{(2m-1)\pi x}{L}\right] \mathcal{I}_m = \kappa_{xy}^q \left\{ 1 - \frac{1 + e^{-L_y/\ell}}{1 + e^{-(L_x+L_y)/\ell}} \exp\left(-\frac{L_x}{2\ell}\right) \cosh \frac{x}{\ell} \right\}. \tag{25}$$

Moreover, we can simplify $\kappa_{xy}^{\text{ph,expt}}(x)$ even further by considering the two opposite limits $L_x \gg \ell$ and $L_x \ll \ell$. In the limit of $L_x \gg \ell$, the second term in the curly brackets of Eq. (25) is negligible, and we find a constant thermal Hall conductivity:

$$\kappa_{xy}^{\text{ph,expt}}(x) = \kappa_{xy}^q. \tag{26}$$

Conversely, in the limit of $L_x \ll \ell$, we can expand the terms in the curly brackets of Eq. (25) up to second order in x/ℓ and L_x/ℓ (while neglecting L_y/ℓ) to obtain a strongly x -dependent thermal Hall conductivity:

$$\kappa_{xy}^{\text{ph,expt}}(x) = \frac{\kappa_{xy}^q(L_x^2 - 4x^2)}{8\ell^2}. \tag{27}$$

Finally, we recover $\kappa_{xy}^{\text{ph,expt}}(x)$ in Eq. (14) of the main text by substituting $\kappa_{xy}^q = (\pi/12)T$ into Eqs. (26) and (27).

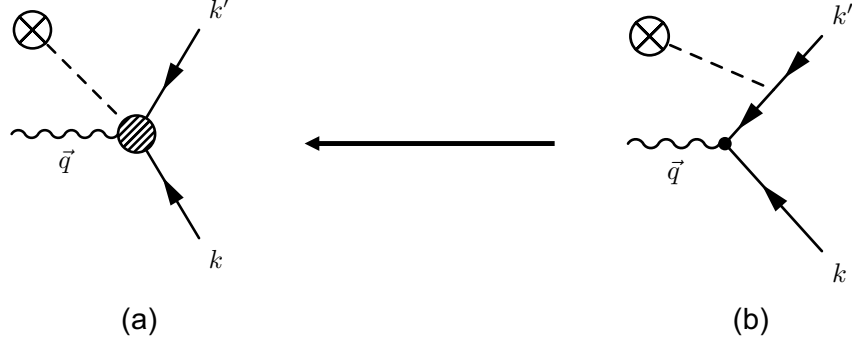


FIG. 3. Diagrammatic representation of the Majorana fermion (solid line) and phonon (wavy line) scattering vertex in the presence of disorder (dashed line with \otimes). (a) The effective Majorana-phonon-disorder vertex presented in Eq. (15). (b) The scattering vertex constructed from the microscopic Majorana-phonon and Majorana-disorder couplings. The connection between the two is shown in Sec. .

Microscopic calculation of the thermal coupling λ

In this section, we start with deriving the linearized energy current between phonons and Majoranas using the Boltzmann equation formalism in Sec. . In Sec. , we justify that the Majorana-phonon-disorder vertex presented in Eq. (15) (see Fig. 3 (a)) of the manuscript can be considered as an effective vertex from the microscopic Majorana-phonon and Majorana-disorder couplings (see Fig. 3 (b)).

Collision integral

We consider the non-interacting Hamiltonians of the Majorana fermion and phonon fields:

$$\mathcal{H}_0 = \frac{-iv_f}{4} \int dx \eta(x) \partial_x \eta(x) + \frac{1}{2} \int dx dy [\rho_0^{-1} \vec{\pi}^2 + B(\vec{\nabla} \cdot \vec{u})^2], \quad (28)$$

where \vec{u} is the lattice displacement field in the continuous limit, $\vec{\pi}$ is the conjugate lattice momentum, ρ_0 is the lattice mass density. The longitudinal phonon field in second quantized form is [20]:

$$\begin{aligned} \vec{u}(\vec{x}, t) &= \sum_{\vec{q}} \left(\frac{\hbar}{2\rho_0 V \omega_{\vec{q}}} \right)^{1/2} \hat{q} \left(c_{\vec{q}} e^{i\vec{q} \cdot \vec{x} - i\omega_{\vec{q}} t} + c_{\vec{q}}^\dagger e^{-i\vec{q} \cdot \vec{x} + i\omega_{\vec{q}} t} \right) \\ \vec{\pi}(\vec{x}, t) &= \rho_0 \frac{\partial \vec{u}}{\partial t} = -i\sqrt{\rho_0} \sum_{\vec{q}} \left(\frac{\hbar \omega_{\vec{q}}}{2V} \right)^{1/2} \hat{q} \left(c_{\vec{q}} e^{i\vec{q} \cdot \vec{x} - i\omega_{\vec{q}} t} - c_{\vec{q}}^\dagger e^{-i\vec{q} \cdot \vec{x} + i\omega_{\vec{q}} t} \right), \end{aligned} \quad (29)$$

where $V = L_x L_y$ is the volume of the system, $\hbar \omega_{\vec{q}}$ the energy of the phonon at momentum \vec{q} , and $\hat{q} = \vec{q}/|\vec{q}|$. In what follows, we consider the majorana-phonon coupling at the *top and bottom* edges only. The Fourier transforms of the Majorana field $\eta(x)$ and of the disorder field along those edges $\zeta(x)$ are

$$\eta(x) = \sqrt{\frac{2}{L_x}} \sum_k \eta_k e^{ikx}, \quad \zeta(x) = \frac{1}{\sqrt{L_x}} \sum_k \zeta_k e^{ikx}, \quad (30)$$

where L_x is the length of the system along the x direction, such that $\{\eta(x), \eta(x')\} = 2\delta(x - x')$, $\{\eta_k, \eta_{k'}\} = \delta_{k, -k'}$, $\langle \zeta(x) \zeta(x') \rangle_{dis} = \zeta^2 \delta(x - x')$, $\langle \zeta_p \zeta_{-p'} \rangle_{dis} = \langle \zeta_p \zeta_{p'}^* \rangle_{dis} = \zeta^2 \delta_{p, p'}$, where $\langle \dots \rangle_{dis}$ denotes a disorder average. \mathcal{H}_0 and the

phonon-Majorana interaction Hamiltonian \mathcal{H}_{int} [from Eq. (15)] in momentum space are

$$\mathcal{H}_0 = \frac{1}{2} \sum_k v_f k \eta_{-k} \eta_k + \sum_{\vec{q}} \hbar \omega_{\vec{q}} c_{\vec{q}}^\dagger c_{\vec{q}} \quad (31)$$

$$\mathcal{H}_{int} = i \frac{g v_f}{4 v_{ph}} \sqrt{\frac{\hbar}{2 \rho_0}} \sqrt{\frac{1}{V L_x}} \sum_{\vec{q}, k, k', p} \sqrt{\omega_{\vec{q}}}(k - k') K_{ij} \hat{q}_i \hat{q}_j \left(\zeta_p c_{\vec{q}}^\dagger \eta_k \eta_{k'} e^{-i q_y y_0} \delta_{p+k+k'-q_x} - \zeta_p c_{\vec{q}} \eta_k \eta_{k'} e^{i q_y y_0} \delta_{p+k+k'+q_x} \right) \quad (32)$$

where $y_0 = L_y/2$, $\omega_{\vec{q}} = v_{ph} \sqrt{q_x^2 + q_y^2}$, with the acoustic phonon velocity $v_{ph} = \sqrt{B/\rho_0}$. Note that the relation $\eta_k = \eta_{-k}^\dagger$ has not been explicitly applied, and the summation over k, k' runs over both negative and positive momenta [but only the annihilation mode η_k appears in Eq. (30)] [21].

The scattering matrix element \mathcal{M}^\pm that *creates*, resp. *annihilates*, a single phonon mode (i.e. which multiplies $c_{\vec{q}}^\dagger \eta_k \eta_{k'}$, resp. $c_{\vec{q}} \eta_k \eta_{k'}$) can be expressed as:

$$\begin{aligned} \mathcal{M}^+(\vec{q}; k, k') &= i \frac{g v_f}{4 v_{ph}} \sqrt{\frac{\hbar}{2 \rho_0}} \sqrt{\frac{1}{V L_x}} K_{ij} \hat{q}_i \hat{q}_j \sqrt{\omega_{\vec{q}}}(k - k') \zeta_{q_x - k - k'} e^{-i q_y y_0} \\ \mathcal{M}^-(\vec{q}; k, k') &= -i \frac{g v_f}{4 v_{ph}} \sqrt{\frac{\hbar}{2 \rho_0}} \sqrt{\frac{1}{V L_x}} K_{ij} \hat{q}_i \hat{q}_j \sqrt{\omega_{\vec{q}}}(k - k') \zeta_{-q_x - k - k'} e^{i q_y y_0}. \end{aligned} \quad (33)$$

To obtain the collision rate of a phonon mode at momentum \vec{q} due to the scattering with Majorana fermions, i.e. $\left(\frac{\partial g(\vec{q})}{\partial t}\right)_{coll}$, we approximate the distribution functions for the phonons and edge Majorana fermions as the thermal distribution of bosons and fermions respectively, with different local temperatures $T + \tilde{T}_{ph}$, $T + \tilde{T}_f$. This approximation should presumably be valid at leading linear order in $\tilde{T}_{ph} - \tilde{T}_f$ since the deviation from the thermal distribution should only contribute at higher orders in $\tilde{T}_{ph} - \tilde{T}_f$. We argue that the system reaches local thermalization due to phonon-phonon and phonon-Majorana scattering. Moreover, given the absence of particle number conservation for either the phonons or Majoranas, the chemical potentials $\mu_{ph,f} = 0$ even away from equilibrium. From Fermi's golden rule, we have

$$\begin{aligned} \left(\frac{\partial g(\vec{q})}{\partial t}\right)_{coll} &= \frac{2\pi}{\hbar} \times 2 \sum_{k, k'} \{ \langle |\mathcal{M}^+(\vec{q}, k, k')|^2 \rangle_{dis} (1 + g_\omega) f_\epsilon f_{\epsilon'} \delta(-\omega_{\vec{q}} + \epsilon_k + \epsilon_{k'}) \\ &\quad - \langle |\mathcal{M}^-(\vec{q}, k, k')|^2 \rangle_{dis} g_\omega f_\epsilon f_{\epsilon'} \delta(\omega_{\vec{q}} + \epsilon_k + \epsilon_{k'}) \} \\ &= \frac{2\pi}{\hbar} \times 2 \sum_{k, k'} \{ \langle |\mathcal{M}^+(\vec{q}, k, k')|^2 \rangle_{dis} (1 + g_\omega) f_\epsilon f_{\epsilon'} \delta(-\omega_{\vec{q}} + \epsilon_k + \epsilon_{k'}) \\ &\quad - \langle |\mathcal{M}^-(\vec{q}, -k, -k')|^2 \rangle_{dis} g_\omega f_{-\epsilon} f_{-\epsilon'} \delta(\omega_{\vec{q}} - \epsilon_k - \epsilon_{k'}) \} \\ &= \frac{2\pi}{\hbar} \times 2 \sum_{k, k'} \{ \langle |\mathcal{M}^+(\vec{q}, k, k')|^2 \rangle_{dis} \mathbb{P}(\omega_{\vec{q}}, \epsilon_k, \epsilon_{k'}) \delta(-\omega_{\vec{q}} + \epsilon_k + \epsilon_{k'}) \}, \end{aligned} \quad (34)$$

where

$$\mathbb{P}(\omega_{\vec{q}}, \epsilon_k, \epsilon_{k'}) = (1 + g_\omega) f_\epsilon f_{\epsilon'} - g_\omega (1 - f_\epsilon) (1 - f_{\epsilon'}), \quad (35)$$

with $g_\omega = 1/(e^{\beta\omega} - 1)$ and $f_\epsilon = 1/(e^{\beta\epsilon} + 1) = 1 - f_{-\epsilon}$. The factor of 2 in front of the summation in Eq. (34) comes from the two ways of creating and annihilating any given Majorana pair. The notation $\epsilon = \epsilon_k$, $\epsilon' = \epsilon_{k'}$, $\omega = \omega_{\vec{q}}$ is used so long as there is no ambiguity (ϵ_k is the Majorana fermion dispersion). The reality of the Majorana mode $\eta(x)$ requires that $\eta_k = \eta_{-k}^\dagger$, thus $\epsilon_k = -\epsilon_{-k}$. From the first to the second line, we take $k \rightarrow -k$, $k' \rightarrow -k'$, i.e. $\epsilon \rightarrow -\epsilon$, which is valid because the summation over k, k' runs over both positive and negative values in our convention. From the second to the last line in Eq. (34), we used the fact that $|\mathcal{M}^+(\vec{q}, k, k')|^2 = |\mathcal{M}^-(\vec{q}, -k, -k')|^2$. The total rate of energy change of the phonon subsystem through the collision with edge Majorana fermions is:

$$\left(\frac{\partial \mathcal{E}}{\partial t}\right)_{ph \rightarrow f} = - \left(\frac{\partial \mathcal{E}_{ph}}{\partial t}\right) = - \sum_{q_x, q_y} \omega_{\vec{q}} \left(\frac{\partial g(\vec{q})}{\partial t}\right)_{coll}, \quad (36)$$

and the heat current from the phonons to the edge Majorana fermions is

$$j_{ex} = \frac{1}{L_x} \left(\frac{\partial \mathcal{E}}{\partial t} \right)_{ph \rightarrow f}.$$

To obtain $\left(\frac{\partial \mathcal{E}}{\partial t} \right)_{ph \rightarrow f}$ at leading order in the temperature difference $\tilde{T}_{ph} - \tilde{T}_f$ (i.e., leading order in $\delta\beta = \beta_f - \beta_{ph}$), we Taylor expand $\mathbb{P}(\omega_{\bar{q}}, \epsilon_k, \epsilon_{k'})$ to $\delta\beta$ order:

$$\mathbb{P}(\omega_{\bar{q}}, \epsilon_k, \epsilon_{k'}) = -\frac{\delta\beta\omega}{2(\sinh\beta\omega - \sinh\beta(\epsilon - \omega) + \sinh\beta\epsilon)} \quad (37)$$

where we made use of the energy conservation relation $\epsilon' = \omega - \epsilon$. For simplicity, we consider isotropic lattice distortions, and take $K_{ij} = \delta_{ij}$ in Eq. (33), so that $\sum_{i,j} K_{ij} \hat{q}_i \hat{q}_j = 1$. Using Eqs. (33,34,37), we find:

$$\begin{aligned} \left(\frac{\partial \mathcal{E}}{\partial t} \right)_{ph \rightarrow f} &= -\frac{2\pi}{\hbar} \frac{\tilde{\Gamma}^2}{VL_x} \sum_{q_x, q_y, k, k'} 2\omega_{\bar{q}} \left(\sqrt{\omega_{\bar{q}}} (\epsilon_k - \epsilon_{k'}) \right)^2 \langle \zeta_{q_x - k - k'} \zeta_{q_x - k - k'}^* \rangle_{dis} \mathbb{P}(\omega_{\bar{q}}, \epsilon_k, \epsilon_{k'}) \times \delta(-\omega_{\bar{q}} + \epsilon_k + \epsilon_{k'}) \\ &= \frac{2\pi}{\hbar} \delta\beta \frac{\tilde{\Gamma}^2 \zeta^2}{VL_x} \frac{L_x}{2\pi v_f} \sum_{q_x, q_y, k} \frac{\omega^3 (2\epsilon - \omega)^2}{\sinh\beta\omega - \sinh\beta(\epsilon - \omega) + \sinh\beta\epsilon} \end{aligned} \quad (38)$$

where $\tilde{\Gamma} = \frac{g}{4v_{ph}} \sqrt{\frac{\hbar}{2\rho_0}}$. From the first to the second line, the summation over k' was performed with the energy conservation $\delta(-\omega_{\bar{q}} + \epsilon_k + \epsilon_{k'})$, contributing a factor $\frac{L_x}{2\pi v_f}$. The sum $\sum_{q_x, q_y, k}$ becomes, in the continuous limit,

$$\sum_{q_x, q_y, k} \rightarrow \frac{L_x^2 L_y}{(2\pi)^3} \int dq_x dq_y dk = \frac{VL_x}{(2\pi)^3 v_{ph}^2 v_f} \int \omega d\omega d\theta_{\bar{q}} d\epsilon. \quad (39)$$

Eq. (38) then becomes:

$$\left(\frac{\partial \mathcal{E}}{\partial t} \right)_{ph \rightarrow f} = \delta\beta \frac{2\pi}{\hbar} \frac{\tilde{\Gamma}^2 \zeta^2}{VL_x} \frac{L_x}{2\pi v_f} \frac{VL_x}{(2\pi)^3 v_{ph}^2 v_f} \int_0^\Lambda d\omega \int_0^{2\pi} d\theta_{\bar{q}} \int_{-\Lambda'}^{\Lambda'} d\epsilon \frac{\omega^4 (2\epsilon - \omega)^2}{\sinh\beta\omega - \sinh\beta(\epsilon - \omega) + \sinh\beta\epsilon}, \quad (40)$$

where Λ and Λ' are the phonon and Majorana fermion energy cutoffs, respectively. From Eq. (40), by power counting energies ω, ϵ , we can already see that the result takes the form of

$$j_{ex} = \frac{1}{L_x} \left(\frac{\partial \mathcal{E}}{\partial t} \right)_{ph \rightarrow f} = \delta\beta \frac{1}{\hbar} \frac{\tilde{\Gamma}^2 \zeta^2}{(2\pi)^3 v_{ph}^2 v_f^2} \left(\frac{1}{\beta} \right)^8 f(v_{ph}/v_f) = \delta\beta \frac{g^2 \zeta^2}{32(2\pi)^3 v_{ph}^4 v_f^2 \rho_0} \left(\frac{1}{\beta} \right)^8 f(v_{ph}/v_f) \sim T^6 (\tilde{T}_{ph} - \tilde{T}_f), \quad (41)$$

where $\delta\beta/\beta^2 = \tilde{T}_{ph} - \tilde{T}_f$. Importantly, from $j_{ex} \sim T^6 (\tilde{T}_{ph} - \tilde{T}_f)$, we can extract the exponent α of the thermal coupling $\lambda(T)$ defined in the main text, i.e., $\alpha = 6$. In passing, we note that without disorder, two-phonon processes are necessary to satisfy kinematic constraints, and one obtains an even larger $\alpha = 8$. The function $f(x)$ in general depends on the ratio of v_{ph}/v_f , and is a dimensionless constant in this model:

$$f = \int_0^\infty du \int_0^{2\pi} d\theta_{\bar{q}} \int_{-\infty}^\infty dv (2v - u)^2 \times \frac{u^4}{\sinh u - \sinh(v - u) + \sinh v} \approx 4.2 \times 10^4, \quad (42)$$

where $u = \beta\omega$, $v = \beta\epsilon$, and at low enough temperature, we take the integration range such that $\Lambda\beta, \Lambda'\beta \rightarrow \infty$. The calculation of f is outlined below. To simplify the integral, we note that the Boltzmann distribution term $\mathbb{P}(\omega, \epsilon, \omega - \epsilon)$ is symmetric around $\epsilon = \omega/2$, so we make the change of variables $v - u/2 \rightarrow \tilde{v}$. The integral measure and range remain unchanged, and the integrand in Eq. (42) becomes

$$f = \int_0^\infty du \int_0^{2\pi} d\theta_{\bar{q}} \int_{-\infty}^\infty d\tilde{v} 4\tilde{v}^2 \frac{u^4}{2 \sinh \frac{u}{2} (\cosh \frac{u}{2} + \cosh \tilde{v})}. \quad (43)$$

The integral over \tilde{v} can be straightforwardly performed using the result:

$$\int_{-\infty}^\infty d\tilde{v} \frac{\tilde{v}^2}{\cosh \tilde{v} + \cosh \ell} = \frac{2\ell(\pi^2 + \ell^2)}{3 \sinh \ell}. \quad (44)$$

Integrating over u , we obtain finally:

$$f = 2\pi \times 160 \times (2\pi^2 \zeta(5) + 21\zeta(7)) \approx 4.2 \times 10^4, \quad (45)$$

where $m \mapsto \zeta(m)$ is the Riemann zeta function.

A more microscopic derivation of the spin-lattice-disorder vertex

In this section, we consider a more generic form of phonon-Majorana coupling (\mathcal{H}_{f-ph}) and disorder-Majorana coupling (\mathcal{H}_{f-dis}) at the edge at $y = y_0 = L_y/2$ as:

$$\begin{aligned}\mathcal{H}_{f-ph} &= \frac{igv_f}{4} \int dx dy K_{ij} \partial_i u_j(x, y) \eta(x) \partial_x \eta(x) \delta(y - y_0), \\ \mathcal{H}_{f-dis} &= \frac{-iv_f}{4} \int dx \zeta(x) \eta(x) \partial_x \eta(x).\end{aligned}\quad (46)$$

Our goal is to justify the disorder vertex taken in Eq. (15) by incorporating the velocity disorder \mathcal{H}_{f-dis} into the vertex disorder $\sim \mathcal{H}_{int}$ by properly rescaling the Majorana field in a way that preserves the anticommutation relation. The quadratic Hamiltonian of the Majorana field is now

$$\mathcal{H}_{quad} = \frac{-iv_f}{4} \int dx (1 + \zeta(x)) \eta(x) \partial_x \eta(x).\quad (47)$$

We define the following canonical transformation of the Majorana field:

$$\eta(x) = \left| \frac{\partial \tilde{x}(x)}{\partial x} \right|^{1/2} \tilde{\eta}(\tilde{x}),\quad (48)$$

for any function $\tilde{x}(x)$ that is invertible, i.e. $\{\tilde{\eta}(\tilde{x}), \tilde{\eta}(\tilde{x}')\} = 2\delta(\tilde{x} - \tilde{x}')$. Considering weak disorder, a natural choice is $\partial \tilde{x}(x)/\partial x > 0$ and $\tilde{x}(x) \rightarrow \pm\infty$ as $x \rightarrow \pm\infty$. In terms of the new coordinate,

$$\eta \partial_x \eta = \left| \frac{\partial \tilde{x}(x)}{\partial x} \right|^2 \tilde{\eta} \partial_{\tilde{x}} \tilde{\eta}, \quad \int dx = \int d\tilde{x} \left| \frac{\partial \tilde{x}(x)}{\partial x} \right|^{-1}.\quad (49)$$

Thus \mathcal{H}_{quad} becomes

$$\mathcal{H}_{quad} = \frac{-iv_f}{4} \int d\tilde{x} (1 + \zeta(x)) \left| \frac{\partial \tilde{x}(x)}{\partial x} \right| \tilde{\eta}(\tilde{x}) \partial_{\tilde{x}} \tilde{\eta}(\tilde{x}).\quad (50)$$

To remove the disorder vertex in \mathcal{H}_{quad} , we require $\left| \frac{\partial \tilde{x}(x)}{\partial x} \right| = \frac{1}{1+\zeta(x)}$. Instead, $\zeta(x)$ appears in the Majorana-phonon vertex as follows:

$$\mathcal{H}_{f-ph} = \frac{igv_f}{4} \int d\tilde{x} dy \frac{K_{ij} \partial_i u_j(x, y)}{1 + \zeta(x)} \tilde{\eta}(\tilde{x}) \partial_{\tilde{x}} \tilde{\eta}(\tilde{x}) \delta(y - y_0).\quad (51)$$

To express $\frac{K_{ij} \partial_i u_j(x, y)}{1 + \zeta(x)}$ in terms of \tilde{x} to leading order in ζ (weak disorder limit),

$$\tilde{x}(x) = \int^x dx' \frac{1}{1 + \zeta(x')} = \int^x dx' (1 - \zeta(x')) + \mathcal{O}(\zeta^2) = x - \int^x dx' \zeta(x') + \mathcal{O}(\zeta^2).\quad (52)$$

The inverse transformation is

$$x(\tilde{x}) = \tilde{x} + \int^{\tilde{x}} dx' \zeta(x') = \tilde{x} + \int^{\tilde{x} + \int^{\tilde{x}} dx'' \zeta(x'')} dx' \zeta(x') = \tilde{x} + \int^{\tilde{x}} dx' \zeta(x') + \mathcal{O}(\zeta^2).\quad (53)$$

For $K_{ij}\partial_i u_j(x, y)$ in terms of $(\tilde{x}, \tilde{y} = y)$, with a careful analysis for $i = x$ and $i = y$ separately at the leading order in ζ :

$$\begin{aligned}
K_{xj}\partial_x u_j(x, y) &= K_{xj}\frac{\partial\tilde{x}}{\partial x}\partial_{\tilde{x}}u_j(x(\tilde{x}), y) = K_{xj}(1 - \zeta(\tilde{x}))\partial_{\tilde{x}}u_j(\tilde{x} + \int^{\tilde{x}} dx'\zeta(x')) \\
&= K_{xj}(1 - \zeta(\tilde{x}))\partial_{\tilde{x}}[u_j(\tilde{x}) + \partial_{\tilde{x}}u_j(\tilde{x})\int^{\tilde{x}} dx'\zeta(x')] \\
&= K_{xj}(1 - \zeta(\tilde{x}))[\partial_{\tilde{x}}u_j(\tilde{x}) + \zeta(\tilde{x})\partial_{\tilde{x}}u_j(\tilde{x}) + \partial_{\tilde{x}}^2u_j(\tilde{x})\int^{\tilde{x}} dx'\zeta(x')] \\
&= K_{xj}(\partial_{\tilde{x}}u_j(\tilde{x}) + \partial_{\tilde{x}}^2u_j(\tilde{x})\int^{\tilde{x}} dx'\zeta(x')), \\
K_{yj}\partial_y u_j(x, y) &= K_{yj}\partial_y u_j(\tilde{x} + \int^{\tilde{x}} dx'\zeta(x')) \\
&= K_{yj}(\partial_y u_j(\tilde{x}) + \partial_{\tilde{x}}\partial_y u_j(\tilde{x})\int^{\tilde{x}} dx'\zeta(x')) \\
&= K_{yj}(\partial_{\tilde{y}}u_j(\tilde{x}) + \partial_{\tilde{x}}\partial_{\tilde{y}}u_j(\tilde{x})\int^{\tilde{x}} dx'\zeta(x')), \tag{54}
\end{aligned}$$

we have $K_{ij}\partial_i u_j(x, y) = K_{ij}(\partial_i u_j(\tilde{x}) + \partial_{\tilde{x}}\partial_i u_j(\tilde{x})\int^{\tilde{x}} dx'\zeta(x')) + \mathcal{O}(\zeta^2)$. The y coordinate in the expression of $u_j(x, y)$ is omitted for brevity so long as there is no ambiguity. To leading linear order in ζ , Eq. (51) is

$$\begin{aligned}
\mathcal{H}_{f-ph} &= \frac{igv_f}{4}\int d\tilde{x} dy K_{ij}\partial_i u_j(x, y)(1 - \zeta(x))\tilde{\eta}(\tilde{x})\partial_{\tilde{x}}\tilde{\eta}(\tilde{x})\delta(y - y_0) \\
&= \frac{igv_f}{4}\int d\tilde{x} dy K_{ij}(\partial_i u_j(\tilde{x}) + \partial_{\tilde{x}}\partial_i u_j(\tilde{x})\int^{\tilde{x}} dx'\zeta(x'))(1 - \zeta(\tilde{x}))\tilde{\eta}(\tilde{x})\partial_{\tilde{x}}\tilde{\eta}(\tilde{x})\delta(y - y_0) \\
&= \frac{igv_f}{4}\int d\tilde{x} dy \left(K_{ij}\partial_i u_j(\tilde{x}) - K_{ij}\partial_i u_j(\tilde{x})\zeta(\tilde{x}) + \partial_{\tilde{x}}(K_{ij}\partial_i u_j(\tilde{x}))\int^{\tilde{x}} dx'\zeta(x') \right) \tilde{\eta}(\tilde{x})\partial_{\tilde{x}}\tilde{\eta}(\tilde{x})\delta(y - y_0). \tag{55}
\end{aligned}$$

Note that the second term in the last line is exactly the disorder vertex in Eq. (15), while the last term is subleading in the limit $v_{ph}/v_f \gg 1$ despite its integral form. To show that, we first specify the boundary condition for the coordinate transformation as $\zeta(\pm\infty) = 0$, and the Fourier transform of the disorder integral in the last term can be well defined

$$\int^{\tilde{x}} dx'\zeta(x') = \int_{-\infty}^{\tilde{x}} dx'\zeta(x') = \frac{1}{\sqrt{L_x}}\sum_p \frac{\zeta_p e^{ip\tilde{x}}}{ip}. \tag{56}$$

The Fourier transform of the last term becomes

$$\begin{aligned}
&\frac{igv_f}{4}\int d\tilde{x} dy \left(\partial_{\tilde{x}}(K_{ij}\partial_i u_j(\tilde{x}))\int^{\tilde{x}} dx'\zeta(x') \right) \tilde{\eta}(\tilde{x})\partial_{\tilde{x}}\tilde{\eta}(\tilde{x})\delta(y - y_0) \\
&= -i\frac{gv_f}{4v_{ph}}\sqrt{\frac{\hbar}{2\rho_0}}\sqrt{\frac{1}{VL_x}}\sum_{\tilde{q}, k, k'} K_{ij}\hat{q}_i\hat{q}_j\sqrt{\omega_{\tilde{q}}}(k - k')\frac{q_x}{q_x - k - k'}\zeta_{q_x - k - k'}e^{-iq_y y_0}c_{\tilde{q}}^\dagger\eta_k\eta_{k'} + h.c., \tag{57}
\end{aligned}$$

which only differs from that of Eq. 33 by a factor $-\frac{q_x}{q_x - k - k'}$. Since $(k + k') = (v_{ph}/v_f)\sqrt{q_x^2 + q_y^2} = (v_{ph}/v_f)q_x/\cos\theta_{\tilde{q}}$ from energy conservation, the factor $-\frac{q_x}{q_x - k - k'} = \frac{\cos\theta_{\tilde{q}}v_f/v_{ph}}{1 - \cos\theta_{\tilde{q}}v_f/v_{ph}} \sim v_f/v_{ph} \ll 1$ for realistic values. This implies that the last term in Eq. (55) with the disorder integral is subleading compared to the disorder vertex discussed in the main text [22].